Electronic Supplementary Material (ESI) for Nanoscale Horizons.
This journal is © The Royal Society of Chemistry 2021

Electronic Supplementary Information

Selective Photocatalytic Production of CH_4 Using Zn-based Polyoxometalate as a Nonconventional CO_2 Reduction Catalyst

Nayeong Kim[ab], Jung Seung Nam[cd], Jinhyeong Jo[a], Junmo Seong[c], Hyunwoo Kim[ab], Youngkook Kwon[be], Myoung Soo Lah[c], Jun Hee Lee[a], Tae-Hyuk Kwon*[cd], Jungki Ryu*[ab]*

[a]Department of Energy Engineering, School of Energy and Chemical Engineering, Ulsan National Institute of Science and Technology (UNIST), 50 UNIST-gil, Ulsan 44919, Republic of Korea

[b]Emergent Hydrogen Technology R&D Center, Ulsan National Institute of Science and Technology (UNIST), 50 UNIST-gil, Ulsan 44919, Republic of Korea

[c]Department of Chemistry, School of Nature Science, Ulsan National Institute of Science and Technology (UNIST), 50 UNIST-gil, Ulsan 44919, Republic of Korea

[d]Center for Wave Energy Materials, School of Natural Science, Ulsan National Institute of Science and Technology (UNIST), 50 UNIST-gil, Ulsan 44919, Republic of Korea

[e]School of Energy and Chemical Engineering, Ulsan National Institute of Science and Technology (UNIST), 50 UNIST-gil, Ulsan 44919, Republic of Korea

*To whom correspondence should be addressed: jryu@unist.ac.kr (J. Ryu), kwon90@unist.ac.kr (T.-H. Kwon), junhee@unist.ac.kr (J.H. Lee)

Table S1 Crystallographic data of ZnPOM.

$K_{10}[Zn_4(H_2O)_2(PW_9O_{34})_2]\cdot 24(H_2O)$	
Formula	$K_{10}Zn_4O_{91.50}P_2W_{18}H_{47}$
Formula weight	5535.09
μ / mm^{-1}	26.967
$D_{calc.}$ / g cm^{-3}	4.449
Crystal System	Monoclinic
Space Group	$P2_1/n$
Colour	White
a / Å	12.283(3)
b / Å	21.373(4)
c / Å	15.622(3)
α / °	90
β / °	92.27(3)
γ / °	90
V / Å^3	4097.9(15)
Z	2
R(reflections)	0.0484
wR_2	0.0977
Parameter	578

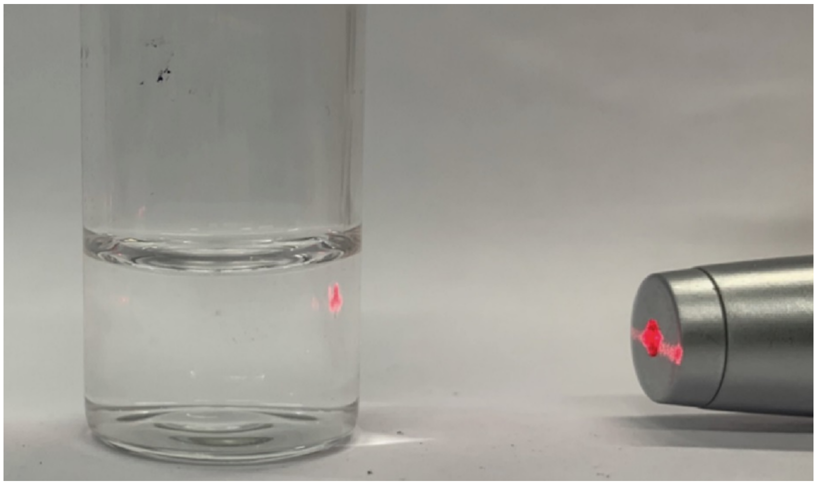

Fig. S1 The Tyndall effect of 30 μM ZnPOM solution in 0.1 M $KHCO_3$.

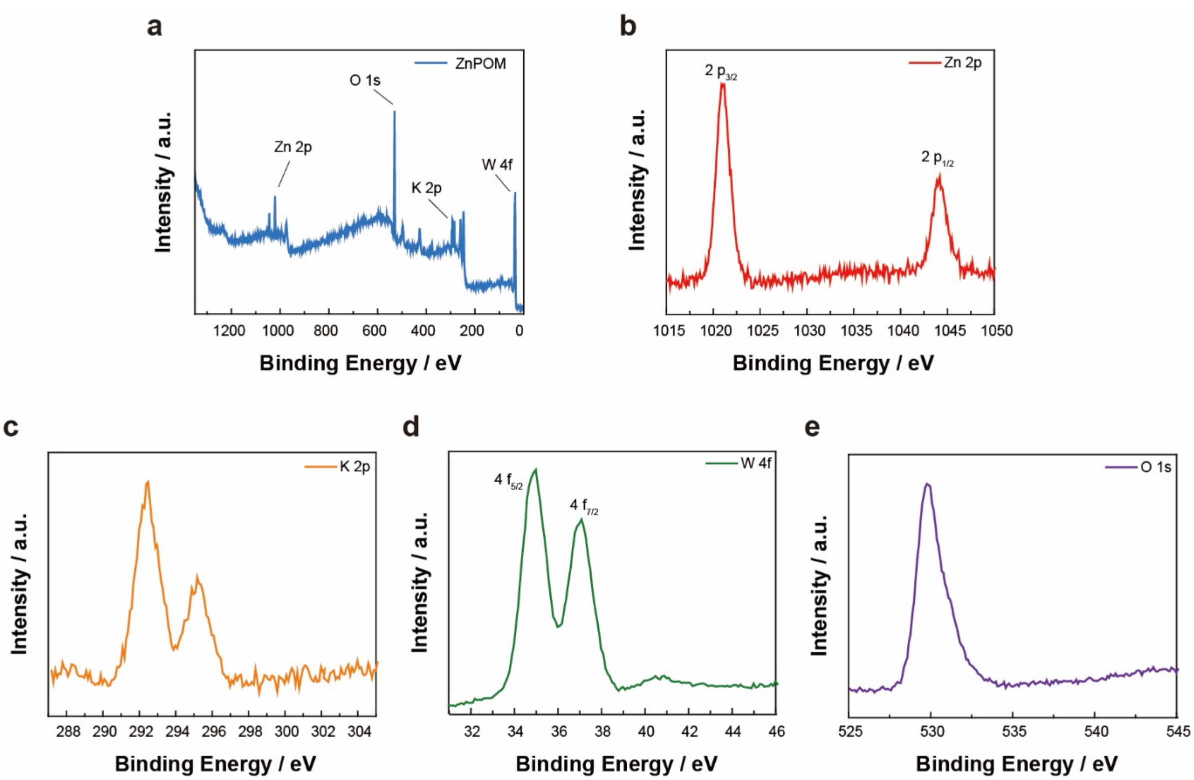

Fig. S2 XPS analysis of ZnPOM. (a) Survey scan, (b) Zn 2p3, (c) K 2p, (d) W 4f, and (e) O 1s spectra of ZnPOM.

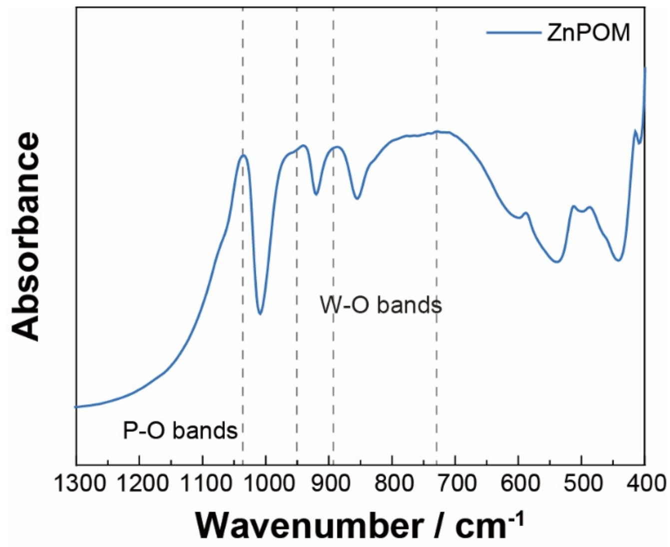

Fig. S3 FT-IR spectrum of ZnPOM in KBr pellet.

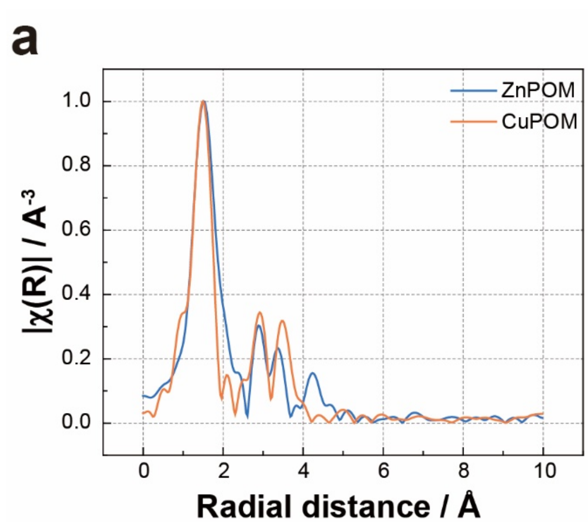

b

(unit : Å)	M-O	M-W1	M-W2
ZnPOM	1.503	2.884	3.374
CuPOM	1.503	2.914	3.466

Fig. S4 EXAFS analysis of ZnPOM and CuPOM: (a) the respective EXAFS spectra, (b) comparison of the distances between Zn (or Cu) and the nearest neighbouring elements in ZnPOM (or CuPOM).

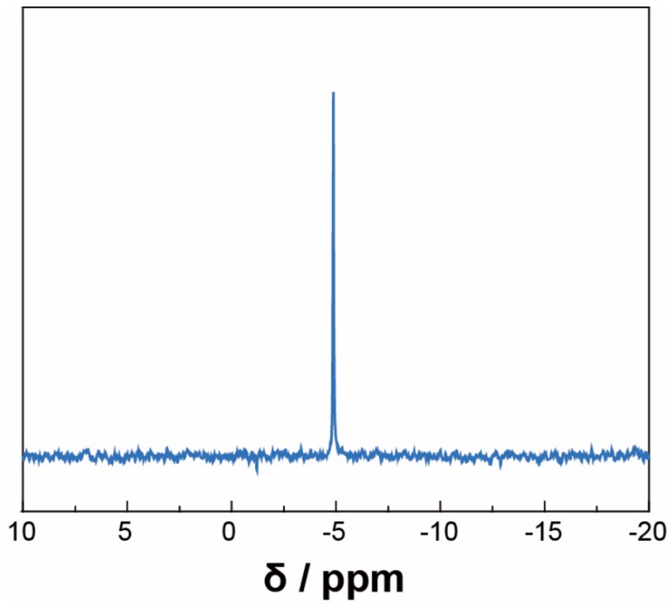

Fig. S5 ^{31}P NMR spectrum of ZnPOM in D_2O solution.

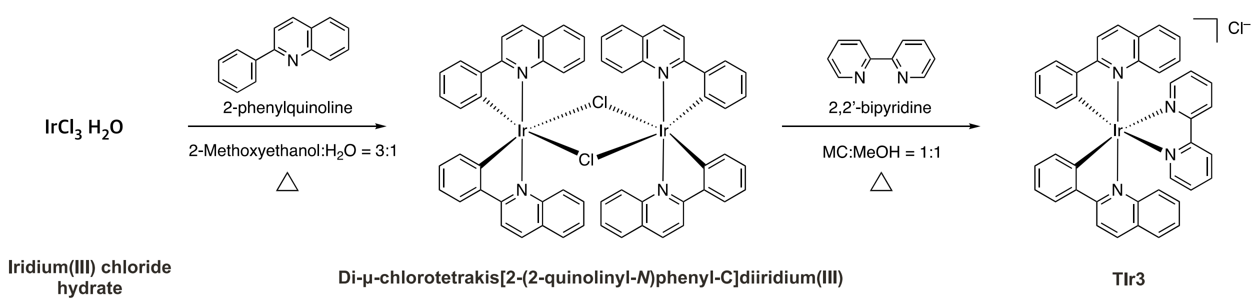

Fig. S6 Synthetic pathway and structure of TIr3.

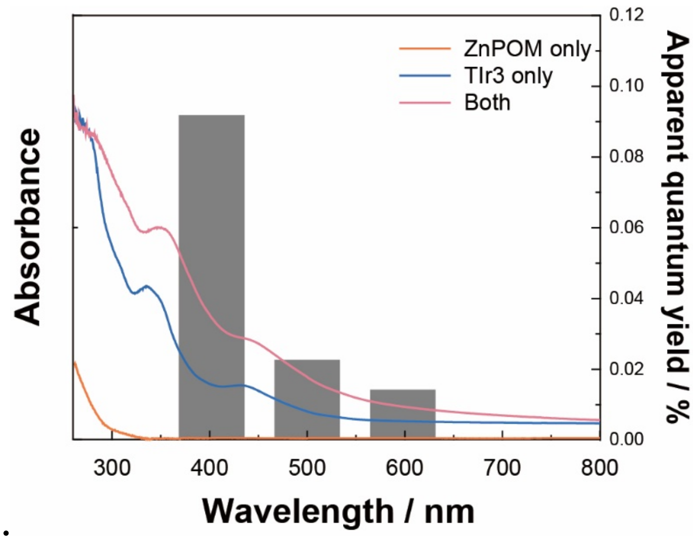

Fig. S7 Apparent quantum yield of photocatalytic CO2RR using ZnPOM and/or TIr3.

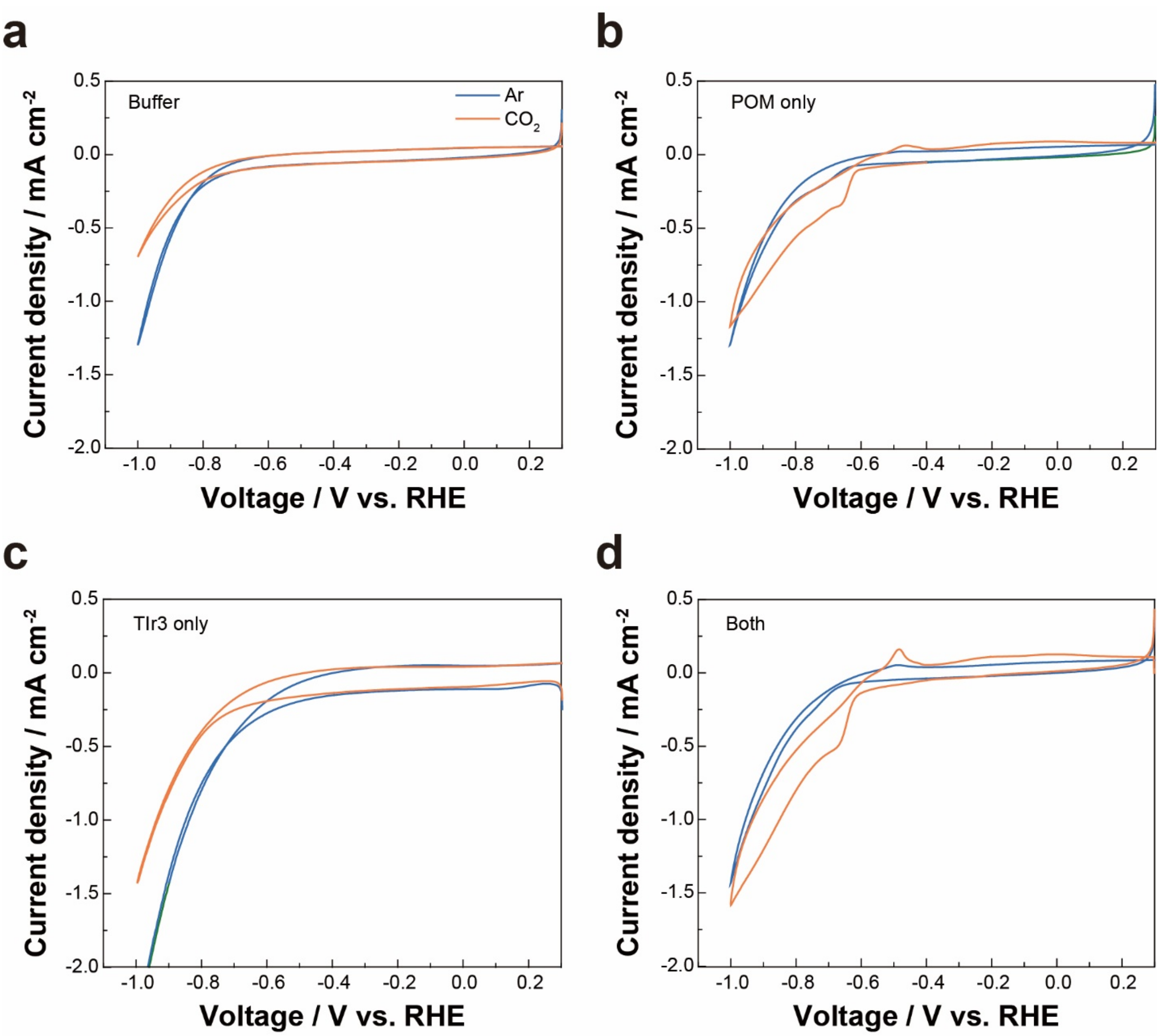

Fig. S8 CV analysis of the respective component in 0.1 M $KHCO_3$ saturated with Ar or CO_2: (a) no component, (b) ZnPOM only (30 μM), (c) TIr3 only (30 μM), and (d) both of them dissolved in 0.1 M $KHCO_3$.

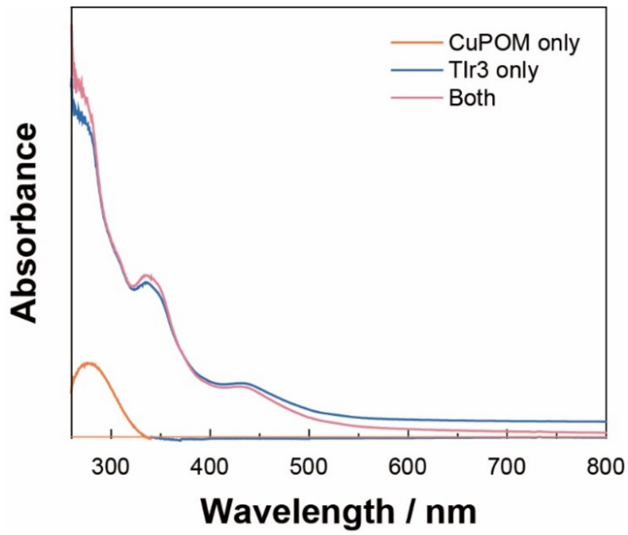

Fig. S9 Absorbance spectra of the respective solutions. The concentration of each component was maintained as a constant: 30 μM CuPOM, 0.1 mM TIr3, and 0.05 M Na_2SO_3 in 0.1 M $KHCO_3$.

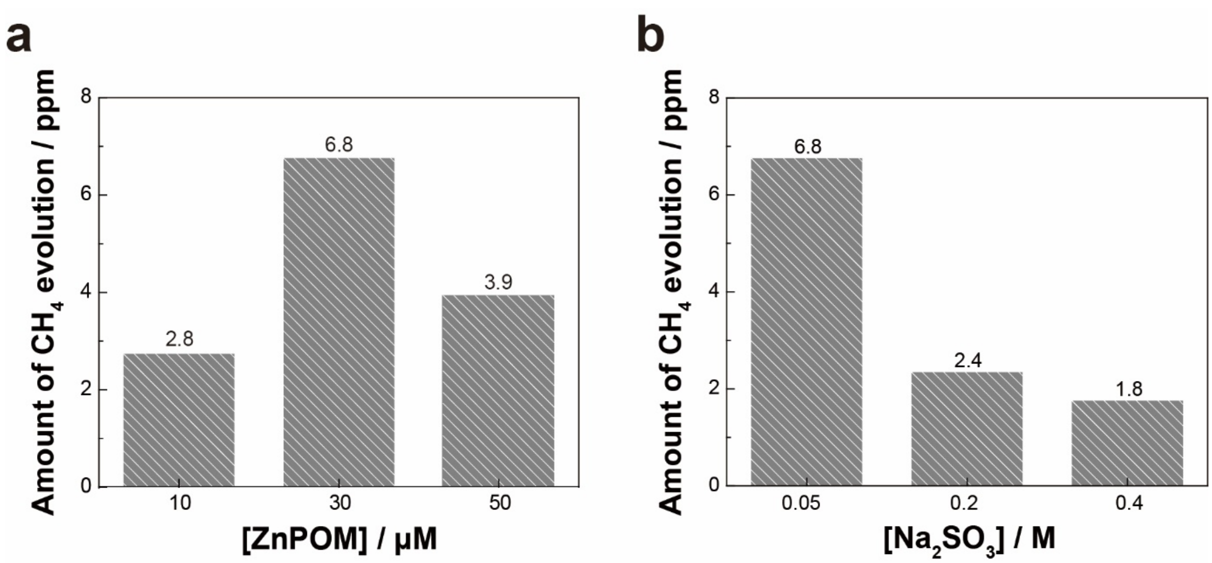

Fig. S10 Optimization of photocatalytic CO2RR conditions using ZnPOM, TIr3, and Na_2SO_3. (a) Amounts of CH_4 produced with different concentrations of ZnPOM. The concentrations of TIr3 and Na_2SO_3 were kept constant at 0.1 mM and 0.05 M, respectively. (b) The amount of CH_4 produced with different concentrations of Na_2SO_3. The concentrations of ZnPOM and TIr3 were kept constant at 30 μM and 0.1 mM, respectively.

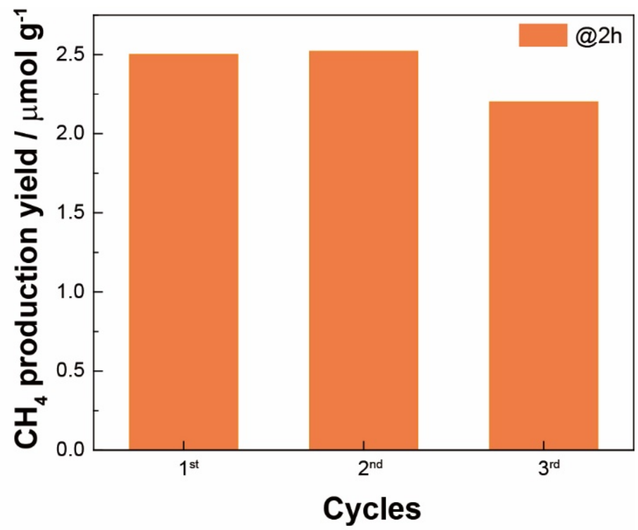

Fig. S11 Recycling test of photocatalytic CO2RR system under visible light irradiation during 2 hours.

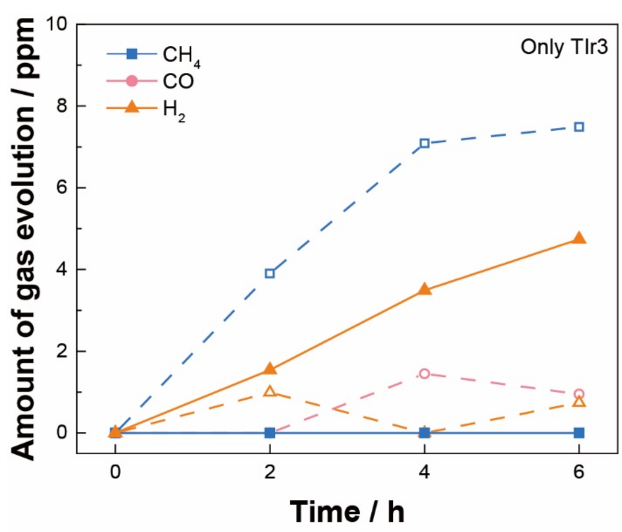

Fig. S12 The effect of ZnPOM on photochemical CO2RR using TIr3 and Na_2SO_3: open symbols and dotted lines, with ZnPOM; closed symbols and solid lines, without ZnPOM.

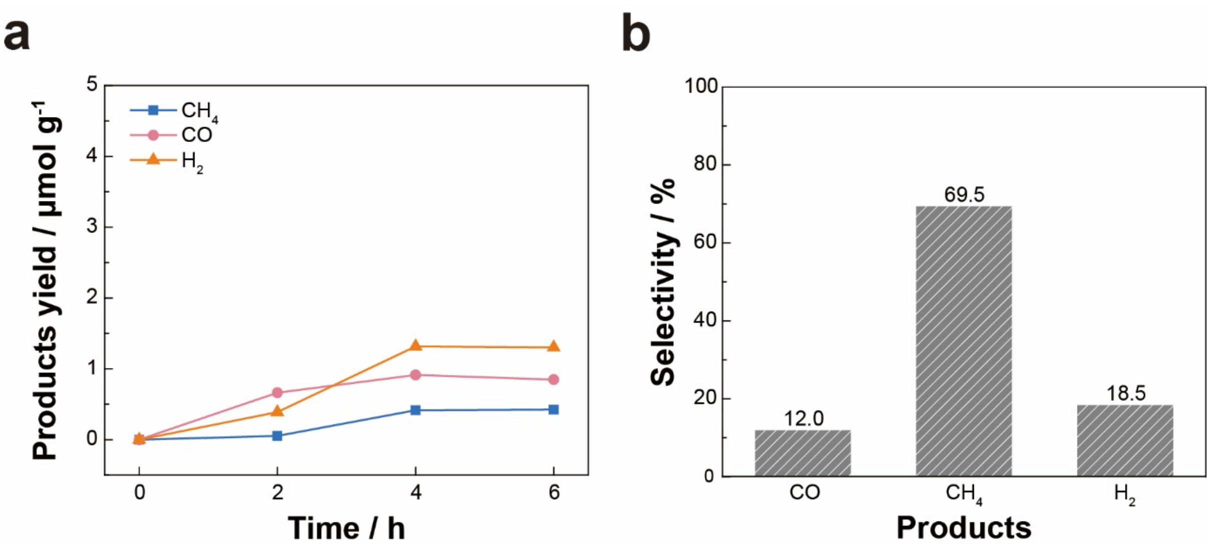

Fig. S13 Photochemical CO2RR using CuPOM. (a) Product yields and (b) selectivity of CO2RR products over time. Photochemical CO2RR was carried out in 0.1 M $KHCO_3$ saturated with CO_2 under the following conditions: 30 μM CuPOM, 0.1 mM TIr3, and 0.05 M Na_2SO_3.

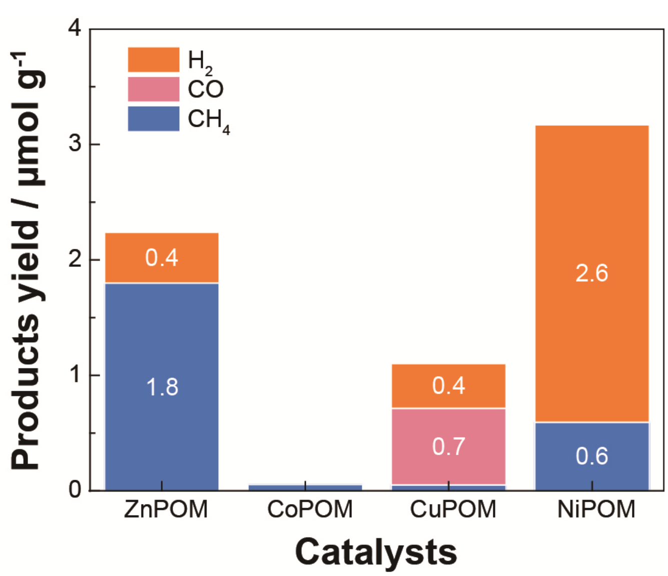

Fig. S14 Photochemical CO2RR using POMs with different metal ions such as Zn, Co, Cu, and Ni (ZnPOM, CoPOM, CuPOM, and NiPOM, respectively). Photochemical CO2RR was carried out for 2 h in 0.1 M $KHCO_3$ saturated with CO_2 under the following conditions: 30 μM POM, 0.1 mM TIr3, and 0.05 M Na_2SO_3.

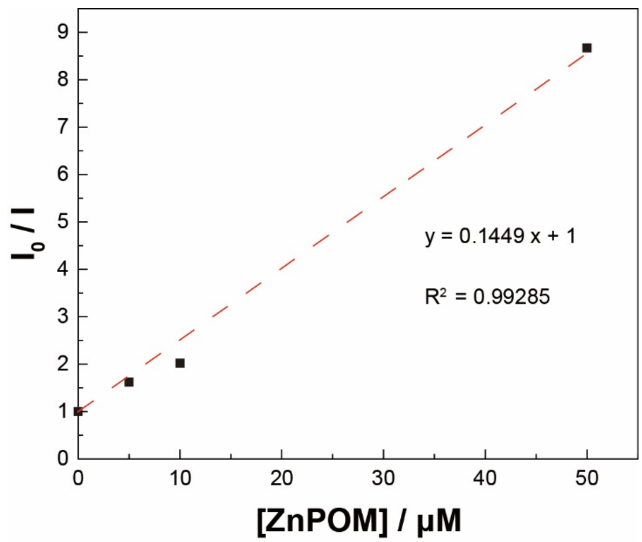

Fig. S15 Stern-Volmer plot for the quenching of TIr3 by ZnPOM.

Table S2 Comparison of performance for CO2RR to CH_4 using various catalysts.

Catalysts	Reaction medium	CH_4 production yield / µmol g^{-1}	Ref.
g-C_3N_4	H_2O vapor	2.55	S1
TiO_2	Isopropyl alcohol	1.2 (5 h)	S2
Cu/TiO_2	CO_2 saturated H_2O	0.024 µmol g^{-1} h^{-1}	S3
CuO-TiO_2	H_2O vapor	2.1 µmol g^{-1} h^{-1}	S4
Cu complex/P-25	H_2O vapor	7 (24 h)	S5
Au/HRTSO	CO_2 and H_2O vapor	5.9 µmol g^{-1} h^{-1}	S6
ZnPOM	**CO_2 saturated 0.1 M $KHCO_3$**	**4.16 (6 h)**	**This work**

Table S3 Comparison of rate constants and bimolecular rate constants in various photocatalytic systems.

	Rate constants, k_q (s^{-1})	**Bimolecular rate constant, K_{sv} (M^{-1} s^{-1})**	**System**	**Target reaction**	**Ref.**
#1	1.2×10^5	$(2.1 \pm 0.4) \times 10^9$	$Ru(bpy)_3^{2+}$ + RuPOM + $Na_2S_2O_8$	OER[a]	S7
#2	8×10^6	8×10^9	Ruthenium complex + Keggin POM	N.A.[b]	S8
	21×10^6	21×10^9	Ruthenium complex + Dawson POM		
#3	N.A.	2.8×10^{11}	$Ru(bpy)_3^{2+}$ MnPOM + TEOA	HER[c]	S9
#4	N.A.	2.7×10^{10}	$[Ir(ppy)_2$ $(dtbbpy)][PF_6]$ + NiPOM + TEOA	HER[c]	S10
#5	N.A.	4.1×10^{10}	$[Ir(ppy)_2(dtbbpy)][PF_6]$ + CuPOM + TEOA	HER[c]	S11
#6	5.84×10^7	1.76×10^{11}	$[Ir(2pq)_2(bpy)][Cl]$: TIr3 + ZnPOM + Na_2SO_3	CO2RR	This work

[a]Oxygen evolution reaction

[b]Not available

[c]Hydrogen evolution reaction

References

S1. W. J. Ong, L. L. Tan, S. P. Chai and S. T. Yong, *Chem. Commun. (Cambridge, U.K.)*, 2015, **51**, 858-861.

S2. S. Kaneco, Y. Shimizu, K. Ohta and T. Mizuno, *J. Photochem. Photobiol. A*, 1998, **115**, 223-226.

S3. D. Liu, Y. Fernández, O. Ola, S. Mackintosh, M. Maroto-Valer, C. M. A. Parlett, A. F. Lee and J. C. S. Wu, *Catal. Commun.*, 2012, **25**, 78-82.

S4. B. Fang, Y. Xing, A. Bonakdarpour, S. Zhang and D. P. Wilkinson, *ACS Sustain Chem. Eng.*, 2015, **3**, 2381-2388.

S5. Y. J. Yuan, Z. T. Yu, J. Y. Zhang and Z. G. Zou, *Dalton Trans.*, 2012, **41**, 9594-9597.

S6. C. Dong, S. Hu, M. Xing and J. Zhang, *Nanotechnology*, 2018, **29**, 154005.

S7. M. Orlandi, R. Argazzi, A. Sartorel, M. Carraro, G. Scorrano, M. Bonchio and F. Scandola, *Chem. Commun.*, 2010, **46**, 3152-3154.

S8. B. Matt, C. Coudret, C. Viala, D. Jouvenot, F. Loiseau, G. Izzet and A. Proust, *Inorg Chem*, 2011, **50**, 7761-7768.

S9. H. Lv, J. Song, H. Zhu, Y. V. Geletii, J. Bacsa, C. Zhao, T. Lian, D. G. Musaev and C. L. Hill, *J. Catal.*, 2013, **307**, 48-54.

S10. H. Lv, W. Guo, K. Wu, Z. Chen, J. Bacsa, D. G. Musaev, Y. V. Geletii, S. M. Lauinger, T. Lian and C. L. Hill, *J. Am. Chem. Soc.*, 2014, **136**, 14015-14018.

S11. H. Lv, Y. Gao, W. Guo, S. M. Lauinger, Y. Chi, J. Bacsa, K. P. Sullivan, M. Wieliczko, D. G. Musaev and C. L. Hill, *Inorg. Chem.*, 2016, **55**, 6750-6758.